Structures 89 (2026) 112105

Contents lists available at ScienceDirect

Structures

journal homepage: www.elsevier.com/locate/istruc

Fragility analysis of high-rise modular buildings with uncertain modal properties equipped with multiple vertically distributed tuned liquid dampers

Hollie Moore, Brian Broderick, Breiffni Fitzgerald, John Hickey*

Department of Civil, Structural and Environmental Engineering, Trinity College Dublin, Dublin, Ireland

HIGHLIGHTS

- Impact of multiple vertically distributed tuned liquid dampers on performance of tall modular structures is considered.
- A reduced-order model is developed to investigate structural response to wind loads.
- Fragility curves demonstrate the effectiveness of MVDTLDs in controlling the dynamic response of high-rise modular buildings.

ARTICLE INFO

Keywords:
Modular construction
Wind-induced acceleration
Reduced-order modelling
Multiple vertically distributed tuned liquid dampers
Fragility analysis

ABSTRACT

Application of modular construction techniques in high-rise structures is becoming increasingly popular. This innovative form of construction is relatively novel, with limited in-situ studies of modular buildings leading to uncertainty surrounding the inherent dynamic properties such as natural frequency and damping ratio. This results in difficulty predicting the dynamic response of high-rise modular buildings reliably and ensuring serviceability limit requirements are satisfied. For any lightweight and flexible high-rise building, serviceability limits can become a governing design criterion. Given the novelty of the construction methodology, there is substantial uncertainty over the modal properties, with outstanding questions about how to effectively predict natural frequency and the inherent level of damping. When uncertainty surrounds the modal properties of a structure, and hence the dynamic response, auxiliary damping can aid in controlling accelerations and ensuring habitability requirements are satisfied. This paper simulates the dynamic response of one of Europe's tallest modular buildings, *Ten Degrees*, located in London, United Kingdom, with the aim of understanding the potential benefits of auxiliary damping in the presence of uncertainty. Both irreducible aleatory uncertainty arising from stochastic wind excitation and initial and reduced epistemic uncertainty in modal properties before and after in-situ monitoring are considered. Multiple Vertically Distributed Tuned Liquid Dampers (MVDTLDs) are employed in the model to assess the improvement in reliability of the structure adhering to ISO 10,137 peak acceleration limits for occupant comfort. Fragility curves are calculated to demonstrate the effectiveness of MVDTLDs in reducing the dynamic response and ensuring occupant comfort despite uncertainty in inherent dynamic properties. MVDTLDs are shown to be an effective control measure, performing more effectively than a single TLD at roof level and improving the reliability of high-rise modular buildings in satisfying habitability requirements.

1. Introduction

Modular construction is a Modern Method of Construction (MMC) which has become increasingly popular due to reported benefits such as speed of construction, improved quality and accuracy, and reduced environmental impact [1–4]. Recent advances in technology, construction methods and computational models have enabled this novel form of construction to be employed in high-rise buildings with heights of over 150 m now realised [5,6]. For high-rise buildings, habitability requirements concerning occupant comfort can become a governing design requirement [7,8]. Standards such as ISO 10,137 set out limits for the acceleration response of buildings related to the natural frequency of the structure [9]. These limits are based on the level of acceleration at which

* Corresponding author.
Email address: john.hickey@tcd.ie (J. Hickey).

https://doi.org/10.1016/j.istruc.2026.112105
Received 31 December 2025; Received in revised form 7 May 2026; Accepted 11 May 2026
Available online 22 May 2026

humans begin to experience discomfort such as trouble concentrating, dizziness and nausea [8,10].

Assessing these habitability criteria can be challenging for tall modular buildings. The novelty of high-rise modular structures results in uncertain dynamic properties with limited research on the stiffness and damping ratios available to inform design [3,11–13]. Finite Element (FE) models of the structure can be used to estimate the natural frequency. However, for modular structures which include a large number of elements, joints and bespoke connections, it can become more difficult to accurately predict the natural frequency using eigenanalysis [2,12,14,15]. Furthermore, estimates of the damping ratio of a structure are based on empirical data obtained through in-situ testing of buildings that employ similar construction methods [16–18]. However, there have been few reported in-situ studies of modular buildings that present estimates of the damping ratio or assess the natural frequency in order to validate FE models. Therefore, there can be significant uncertainty in estimates of the modal properties of high-rise modular buildings leading to difficulty ensuring serviceability limits are satisfied [11,19].

These issues emerged during the design of one of Europe's tallest modular buildings, *Ten Degrees*, located in Croydon, London, United Kingdom, as reported in [19,21]. Pictured in Fig. 1, this is a 135 m tall development with volumetric modules stacked around cast in-situ reinforced concrete cores. As discussed in detail in [21], during the design process of *Ten Degrees*, uncertainty in the dynamic behaviour of the structure due to the novelty of this form of construction, led to concerns that the wind-induced acceleration response of the structure would not satisfy habitability requirements. Furthermore, the stiffness contribution of the modules was unknown and assumed to be negligible, resulting in the FE models of *Ten Degrees* underestimating the natural frequency of the structure compared to values obtained from in-situ monitoring. This led designers to consider suitable methods for controlling potentially excessive vibrations. Ultimately, through in-situ testing, the real dynamic behaviour of *Ten Degrees* was captured and the designers decided that no additional control methods were necessary [21]. However, as modular structures continue to increase in height, and for the future progress of this novel form of construction, it is imperative to assess suitable methods to control the wind-induced vibration response.

Tuned Liquid Dampers (TLDs) have been proven to be an effective vibration control method for tall, flexible structures with reported advantages including simple configuration, low maintenance, low installation cost and reduced space requirements compared to Tuned Mass Dampers [22–26]. The most basic form of a TLD involves a tank filled with water to a specified depth so that when excited the water sloshes at a frequency close to that of the structure with the aim of mitigating excessive vibrations. However, other configurations of TLDs have been explored such as including baffles or screens within the tank to further aid energy dissipation [27–29]. Furthermore, many studies have shown that Multiple Tuned Mass Dampers (MTMDs) can be more effective in controlling the dynamic response of a structure than a single TMD [30–35]. MTMDs enable a greater range of modes of a structure to be controlled as the individual TMDs can be tuned to the different natural frequencies of the structure [33]. Moreover, TMDs can be vertically distributed throughout the height of a building, with consideration given to the mode shapes of the structure when the optimal TMD locations and tuning frequencies are designed [36]. Despite the advantages of TLDs over TMDs, there have been limited studies on multiple distributed TLDs.

Conventional TLD implementation at present involves a single damper, typically near the top of a building. However, the concept of multiple distributed TLDs is appealing in the context of modular construction for a number of reasons. From the point of view of maximising the TLD performance, the optimum ratio of the depth of liquid in TLDs to the length of the TLD is generally less than 0.3, with studies demonstrating that as this ratio increases, damping decreases [37]. Therefore, to achieve significant damping and mass ratios whilst still tuning TLDs to the fundamental frequency of the primary structure, it is potentially more advantageous to use multiple smaller TLDs than one large TLD. Hence, distributing multiple small TLDs throughout a structure is a practical control strategy which capitalises on the optimum design of TLDs. This concept becomes practically achievable for modular construction, where similar modules are typically fabricated on an assembly line in a factory. The repeatable nature of the individual units in modular buildings is well suited to the idea of distributing the TLDs throughout the structure, including vertically over a number of storeys. Therefore, Multiple Vertically Distributed Tuned Liquid Dampers, or MVDTLDs, appear to be well suited to the form of modular construction, taking advantage of the flexibility and repeated nature of the design. Fig. 2 shows how a number of damping devices can be distributed vertically over a structure. This idea distributes the space requirements of supplementary

(a) During construction

(b) Completed

Fig. 1. The *Ten Degrees* development, the source of the data in this paper, pictured (a) during module installation and (b) after completion [20].

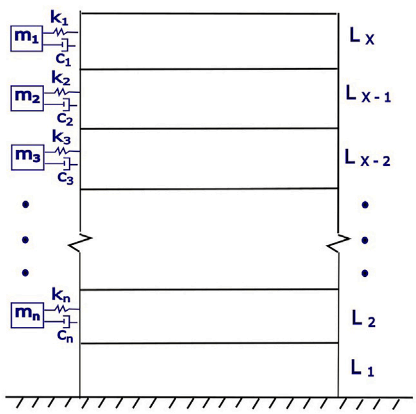

Fig. 2. Multiple damping devices distributed vertically along the height of a structure.

damping devices and could be easily included in the off-site manufacturing of volumetric modules. This could be achieved by, for example, devoting a single module to house multiple TLDs on each of the upper storeys of a modular building or by installing a small TLD in every module at specified storeys.

In the case of modular construction, where uncertainty surrounds the dynamic properties, supplementing the inherent damping with auxiliary devices such as TLDs or MVDTLDs can potentially help to provide certainty that the dynamic response is controlled and that habitability requirements are met [38]. The addition of auxiliary damping devices results in the possible range in the estimate of the inherent damping becoming a smaller fraction of the total damping of the system [39]. This reduces the overall uncertainty in the acceleration response; thus offering a potential solution to the challenge of ensuring serviceability limits are satisfied under uncertain modal properties. There are few studies examining the reliability enhancement of structural response with the use of auxiliary damping devices [40], particularly for SLS design considering the ability of dynamic performance to meet habitability requirements. With this in mind, the aim of this work is to develop fragility curves for a 45 storey modular building which compare the probability of exceeding ISO 10,137 [9] habitability criteria with uncertain levels of natural frequency and damping ratio with and without MVDTLDs. A reduced-order model of the *Ten Degrees* building is developed to calculate the wind-induced peak acceleration response of the modular high-rise building. An initial 'uninformed' analysis is performed employing modal properties obtained using Eurocode recommended methods and empirical estimates of errors in these estimates. A second 'data-informed' analysis is performed using modal properties identified through in-situ testing and application of Operational Modal Analysis methods as described by Hickey et al. in [19]. For both the initial and informed cases the dynamic response of the structure both in its uncontrolled state without TLDs and in its controlled state with MVDTLDs is assessed using a number of simulations at different wind speeds and the peak acceleration response is compared to ISO 10,137 limits for human comfort. Fragility curves are generated and used to assess the performance of supplementary damping devices in the presence of epistemic uncertainty. The developed fragility curves provide a useful tool for investigating the enhancement of the reliability of high-rise modular structures satisfying serviceability requirements when equipped with supplementary damping devices.

2. Reduced-order modelling

In structural engineering it is common to use reduced-order models, such as equivalent beam models or lumped mass models with a small number of degrees of freedom, as surrogates to represent a complex structure in order to predict the dynamic response [41]. Given their computational simplicity compared to large FE models, these surrogate models can be particularly useful when performing parametric assessments, uncertainty quantification or investigating the effectiveness of supplementary damping devices in increasing the reliability of a structure. Therefore, in this paper a reduced-order model considering the first mode of vibration and variable distribution of Tuned Liquid Dampers of *Ten Degrees* is created in order to investigate control of the dynamic response with auxiliary damping devices.

2.1. Multi degree of freedom modelling using modal superposition methods

The fundamental equation of motion for a Multi Degree of Freedom (MDOF) System is:

$$\boldsymbol{M}\ddot{\boldsymbol{x}}(t) + \boldsymbol{C}\dot{\boldsymbol{x}}(t) + \boldsymbol{K}\boldsymbol{x}(t) = \boldsymbol{p}(t) \tag{1}$$

where **M**, **C** and **K** are the mass, damping and stiffness matrices representing each DOF, $\ddot{x}(t)$, $\dot{x}(t)$ and $x(t)$ are vectors of the acceleration, velocity and displacement response of each DOF and $p(t)$ is a time-history of the forces applied at each DOF. In this paper, one DOF is defined for each storey of the structure.

Using the standard modal transformation $\boldsymbol{x} = \boldsymbol{\phi} q$, the structure can be analysed in modal coordinates:

$$\ddot{q}_i(t) + 2\zeta_i\omega_{n,i}\dot{q}_i(t) + \omega_{n,i}^2 q_i(t) = \frac{p^*(t)}{\boldsymbol{M}_i^*} \tag{2}$$

where $\ddot{q}_i(t)$, $\dot{q}_i(t)$ and $q_i(t)$ are the i^{th} modal acceleration, velocity and displacement responses and M_i^* is the i^{th} modal mass, calculated as $\boldsymbol{\phi}_i^T \mathbf{M} \boldsymbol{\phi}_i$. ζ_i is the critical damping ratio and $\omega_{n,i}$ is the natural frequency in the i^{th} mode. $p^*(t)$ is the modal force calculated as $\boldsymbol{\phi}_i^T \mathbf{p}$. In this form of the equation, all variables can be informed by the properties in Table 2 considering only the first mode, which is regularly assumed to be sufficient to predict wind-induced response of structures of this scale (e.g. [42,43]). The first mode shape vector, $\boldsymbol{\phi}_1$, can be approximated using Eq. (3), which Eurocode 1991-1-4 [44] recommends 'for slender cantilever buildings and buildings supported by central reinforced concrete cores.'

$$\boldsymbol{\phi}_{j1} = \left(\frac{z_j}{h}\right)^{1.5} \tag{3}$$

Here z_j is the height of the j^{th} DOF above ground and h is the total height of the building.

2.2. Multiple vertically distributed tuned liquid dampers

To incorporate MVDTLDs in the data-informed MDOF reduced-order model, the equivalent Tuned Mass Damper (TMD) model of a TLD proposed by Sun et al. [45] and further developed by Tait [37] is employed. The equivalent TMD properties of the TLDs can be used to represent the TLDs at the relevant DOFs within the surrogate model. The reduced-order model has been developed to accommodate any number of TLDs added to any storey over the height of the structure. Where multiple TLDs are located on one storey, the properties are lumped at that DOF.

Table 1
Properties of TLDs used in data-informed surrogate model.

Property	Value
Storeys TLDs installed	31 - 45
Number of TLDs per Storey	15
TLD Length, L	2.5 m
TLD Width, b	2 m
TLD Depth	0.5 m
Liquid Depth, h	0.26 m
Tuning Ratio, Ω	1
Total Mass Ratio, μ	2.5%

Table 2
Properties of *Ten Degrees* used in the data-informed reduced-order MDOF model.

Building Parameter	Uninformed Case	Data-informed Case
Building height	135 m	
Building width	41 m	
Building depth	44 m	
Mass per meter height	263,737.7 kg/m	
Mean F_1	0.316 Hz	0.3131 Hz
CoV F_1	0.25	0.015
Mean ζ_1	1.27%	1.33%
CoV ζ_1	0.5	0.091

The equivalent TMD model proposed by Tait [37] uses equivalent natural frequency, ω_{eq}, mass, m_{eq}, stiffness, k_{eq}, and damping ratio, ζ_{eq}, values to model the behaviour of the TLD. These values are calculated based on the tank length, L, width, b, liquid height, h, liquid density, ρ, and the kinematic viscosity of the fluid, v, as shown in Eqs. (4)-(8).

$$\omega_{eq} = \frac{\pi g}{L} tanh(\frac{\pi h}{L}) \tag{4}$$

$$m_{eq} = \frac{8\rho b L^2}{\pi^3} tanh(\frac{\pi h}{L}) \tag{5}$$

$$k_{eq} = \frac{8\rho b L g}{\pi^2} tanh^2(\frac{\pi h}{L}) \tag{6}$$

$$\zeta_{eq} = \frac{1}{2h}\sqrt{\frac{v}{2\omega_n}}(1 + \frac{2h}{b} + SC) \tag{7}$$

$$c_{eq} = \zeta_{eq} 2 m_{eq} \omega_{eq} \tag{8}$$

where SC is a surface contamination factor which is taken as 1 [37]. To maximise the performance of the TLD, the mass ratio, μ, of the TLD equivalent mass, m_{eq} to the modal mass, M^*, is defined as in Eq. (9):

$$\mu = \frac{m_{eq}}{M^* + \rho b h L - m_{eq}} \tag{9}$$

The value of the mass ratio, μ, typically lies between 0.5% and 5% [22, 45,46], with a larger value providing more supplemental damping. The relationship between damping ratio, ζ, and the mass ratio, μ, is shown in Eq. (10).

$$\zeta_{eff} = \frac{1}{4}\sqrt{\frac{\mu + \mu^2}{1 + \frac{3\mu}{4}}} \tag{10}$$

The size of the TLD can be chosen in order to maximise μ or to achieve the desired level of supplemental damping. However, in some cases, such as with modular structures, it is potentially more efficient to use multiple TLDs to maintain the optimum ratio of the liquid depth to the TLD length, h/L as less than 0.3 [37].

It is important that the TLDs are tuned to the frequency of the vibration mode to be suppressed. The tuning ratio, Ω, is the ratio of the natural frequency of the TLD, ω_{eq}, to the natural frequency of the structure, ω_s. To optimise the performance of a TLD, this value is chosen as close to 1 as possible [37,47,48].

$$\Omega = \frac{\omega_{eq}}{\omega_s} \tag{11}$$

The equivalent values, mass ratio and tuning ratio outlined above are used to represent the MVDTLDs in the data-informed surrogate model. The mass, stiffness, damping and force matrices are modified as shown in Eqs. (12) to (15).

$$\underbrace{\begin{bmatrix} M^* & 0 & 0 & \cdots & 0 \\ 0 & m_{\text{eq},1} & 0 & \cdots & 0 \\ 0 & 0 & m_{\text{eq},2} & \cdots & 0 \\ \vdots & \vdots & \vdots & \ddots & \vdots \\ 0 & 0 & 0 & \cdots & m_{\text{eq},P} \end{bmatrix}}_{\mathbf{M}} \begin{bmatrix} \ddot{q}(t) \\ \ddot{x}_1(t) \\ \ddot{x}_2(t) \\ \vdots \\ \ddot{x}_P(t) \end{bmatrix} \tag{12}$$

$$+ \underbrace{\begin{bmatrix} C^* + \sum_{j=1}^{P} c_{\text{eq},j}\phi_{j1}^2 & -\phi_{11}c_{\text{eq},1} & -\phi_{21}c_{\text{eq},2} & \cdots & -\phi_{P1}c_{\text{eq},P} \\ -\phi_{11}c_{\text{eq},1} & c_{\text{eq},1} & 0 & \cdots & 0 \\ -\phi_{21}c_{\text{eq},2} & 0 & c_{\text{eq},2} & \cdots & 0 \\ \vdots & \vdots & \vdots & \ddots & \vdots \\ -\phi_{P1}c_{\text{eq},P} & 0 & 0 & \cdots & c_{\text{eq},P} \end{bmatrix}}_{\mathbf{C}} \begin{bmatrix} \dot{q}(t) \\ \dot{x}_1(t) \\ \dot{x}_2(t) \\ \vdots \\ \dot{x}_P(t) \end{bmatrix} \tag{13}$$

$$+ \underbrace{\begin{bmatrix} K^* + \sum_{j=1}^{P} k_{\text{eq},j}\phi_{j1}^2 & -\phi_{11}k_{\text{eq},1} & -\phi_{21}k_{\text{eq},2} & \cdots & -\phi_{P1}k_{\text{eq},P} \\ -\phi_{11}k_{\text{eq},1} & k_{\text{eq},1} & 0 & \cdots & 0 \\ -\phi_{21}k_{\text{eq},2} & 0 & k_{\text{eq},2} & \cdots & 0 \\ \vdots & \vdots & \vdots & \ddots & \vdots \\ -\phi_{P1}k_{\text{eq},P} & 0 & 0 & \cdots & k_{\text{eq},P} \end{bmatrix}}_{\mathbf{K}} \begin{bmatrix} q(t) \\ x_1(t) \\ x_2(t) \\ \vdots \\ x_P(t) \end{bmatrix} \tag{14}$$

$$= \begin{bmatrix} p^*(t) \\ 0 \\ 0 \\ \vdots \\ 0 \end{bmatrix} \tag{15}$$

where the subscripts 1 to P represent the DOFs where a TLD is located and C^* and K^* are defined as in Eqs. (16) and (17).

$$K^* = M^* \omega_n^2 \tag{16}$$

$$C^* = 2\zeta M^* \omega_n \tag{17}$$

Previous studies have shown that distributing TLDs based on the mode shape can be as effective as standard approaches of locating all TLDs at the top of the structure [36,49]. In light of this, a preliminary investigation was performed to establish a suitable distribution of MVDTLDs. Seven different distribution scenarios were considered in which the same number of TLDs, with the same properties, were distributed throughout the structure. The number of TLDs and their properties were kept constant to ensure the mass ratio was consistent across scenarios and that each TLD was tuned to the fundamental frequency of the structure. The methods outlined in Section 2.3 were performed to calculate the median peak acceleration response of the structure in each distribution scenario with a basic wind speed, v_{b0} of 21 m/s which is the value recommended by Eurocode 1-1-4 and the British National Annex for a wind event with a return period of 50 years. The building parameters used were those listed in Table 2 for the uninformed case and the TLD properties are those listed in rows 3–8 of Table 1. For each distribution scenario, the peak acceleration response to 100 wind time histories was calculated and the median value was calculated to account for aleatory uncertainty. The median peak acceleration for each distribution strategy was compared to that of the uncontrolled structure with no auxiliary damping and the percentage reduction in peak acceleration response was calculated. The percentage reduction in peak acceleration is presented in Fig. 3. It is observed that the maximum reduction occurs when MVDTLDs are distributed over the top third of the building. From this, it was concluded that a distribution of MVDTLDs over storeys within the top third of the structure was the best performing configuration. Therefore, this distribution configuration was considered for further analysis.

2.3. Simulation of along-wind loads

Time histories of along-wind forces at each floor level are calculated as the sum of a mean and fluctuating component. The force, $p(z,t)$, which

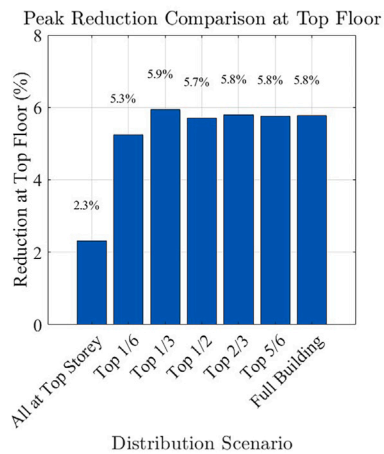

Fig. 3. Reduction in peak acceleration response at the top storey under different distribution strategies.

varies with both time and height, is calculated as:

$$p(z,t) = 0.5C_D \rho A v_m(z)^2 + C_D \rho A v_m(z) u(z,t) \tag{18}$$

where C_D is the drag coefficient, ρ is the density of air, A is the cross-sectional area taken as storey height by building width, $v_m(z)$ is the mean wind speed at height z, $u(z,t)$ is the variable component of the wind speed at height z and time t. The drag coefficient is calculated based on the approach presented for structures with rectangular cross sections in Eurocode 1991-1-4, which for the dimensions of the case study building here results in a value of $C_D = 1$. The mean wind speed at height z is given by the logarithmic law applied in Eurocode 1991-1-4:

$$v_m(z) = 0.19 \frac{z_0}{0.05} \ln\left(\frac{z}{z_0}\right) v_{b0} \tag{19}$$

where the basic wind velocity, v_{b0}, is the 10 minute mean wind velocity at 10 m above ground level in open country and z_0 is the roughness length, given as $1m$ for urban areas in Eurocode 1991-1-4.

A time history representing the variable component of the wind speed, $u(z,t)$, is generated using the methodology proposed by Wittig and Sinha to simulate a multi-correlated random process [50]. This process involves first generating a vector of ns Gaussian complex numbers at each frequency, $\epsilon(f) = \xi + i\eta$, such that ξ and η have a mean of zero and a variance of 0.5. This is then used to generate a frequency domain representation of the fluctuating wind speed at height z_i:

$$U(z_i, f) = \sum_{k=1}^{ns} G_{i,k}(f) \epsilon_k(f) \sqrt{2 f_c N} \tag{20}$$

where f_c is the Nyquist frequency (which is dictated by the time step, which is chosen as $0.03s$), N is the total number of points to be simulated and ns is the number of storeys, 45 in this case. $G_{i,k}(f)$ is the Cholesky decomposition of the cross power spectral density matrix at frequency f representing the random process to be synthesized, which in this case is the normalized Kaimal wind velocity spectrum presented in Eurocode 1991-1-4. The diagonal terms of this matrix are defined as:

$$S_v(z_i, f) = \frac{6.8 \frac{f L(z_i)}{v(z_i)}}{(1 + 10.2 \frac{f L(z_i)}{v(z_i)})^{\frac{5}{3}}} \tag{21}$$

where $v(z_i)$ is the mean wind speed at height z_i calculated using Eq. (19) and $L(z_i)$ is the turbulence length scale at z_i given as:

$$L(z_i) = \max\left(300 \frac{z_i}{200}^{0.67+0.05ln(z_0)}, 34.7\right) \tag{22}$$

Off-diagonal terms in the cross power spectral density matrix are calculated as:

$$S_v(z_i, z_j, f) = \sqrt{S_v(z_i, f) S_v(z_j, f)} coh(z_i, z_j, f) \tag{23}$$

where the coherence function between z_i and z_j is defined as:

$$coh(z_i, z_j, f) = \exp\left(-\frac{2 f c_z |z_i - z_j|}{v_m(z_i) + v_m(z_j)}\right) \tag{24}$$

where c_z is the decay coefficient, taken as 11.5 as per Eurocode 1991-1-4. Eqs. (21) and (23) are used to construct the cross power spectral density matrix, which in turn is used to obtain the $G_{i,k}(f)$ term in Eq. (20). Once Eq. (20) has been evaluated for all frequencies, a discrete inverse Fourier transform can be performed to obtain a time history, $u(z,t)$. An example of a generated time history and power spectral density at roof level for a basic wind velocity of $15m/s$ is presented in Fig. 4, where it can be appreciated that the frequency content of the generated wind speed matches the target spectrum.

The along-wind loading is calculated for a time period of ten minutes plus some time, set equal to three decay constants for the structure in question, to accommodate removal of the transient response to ensure statistical stationarity. The time-history of wind forces are applied to the model as $\boldsymbol{p}(t)$ in Eq. (15) to calculate the wind-induced dynamic response of the structure. The Newmark Beta numerical integration method, using the standard constant average acceleration approach with $\gamma = 0.5$ and $\beta = 0.25$, is used to solve Eq. (15) for the acceleration, velocity and displacement response at each step of the wind loading time history. The transient response of the system can then be removed from the beginning of each of the responses leaving a remaining 10-minute dynamic response.

2.4. Model validation

The reduced-order modelling approach discussed above was validated using the CAARC building, which is widely used as a benchmark in wind engineering (e.g. [52–54]). This example building was originally selected by the Commonwealth Advisory Aeronautical Research Council (CAARC) of Australia in 1980 as a benchmark high-rise structure to be employed for studying wind-induced dynamic response [51]. The full-scale building is a prismatic structure of height 183 m with a rectangular floor plan of dimensions breadth 30.5 m and depth 45.7 m. This building was employed here as the recorded wind speed data from *Ten Degrees* is not sufficient for validation. Dynamic properties of the CAARC building, including first mode natural frequency of 0.2 Hz and damping of 1%, used as model inputs were obtained from previous work by Smith and Caracoglia [43]. 100 different wind speed time histories were generated in accordance with the procedure described in Section 2.3 and applied to the modelled structure. The mean root mean square along-wind acceleration response across these 100 analyses is compared with wind-tunnel-based experimental results reported from a series of aeroelastic wind tunnel tests [51]. As can be seen in Fig. 5, results from the proposed reduced-order model closely replicate the benchmark results. Thus the modelling approach is deemed appropriate for further analysis, including the investigation of the impact of MVDTLDs.

2.5. Consideration of aleatory and epistemic uncertainty

When modelling modular buildings, the modal properties, namely the natural frequency and damping ratio, are considered to be epistemically uncertain; that is they are uncertain due to a lack of knowledge but the extent of this uncertainty can be reduced as more information becomes available. On the other hand the stochastic wind excitation is also uncertain, but in an aleatory sense as it arises from inherent randomness in the turbulent wind field. This represents an irreducible form of uncertainty.

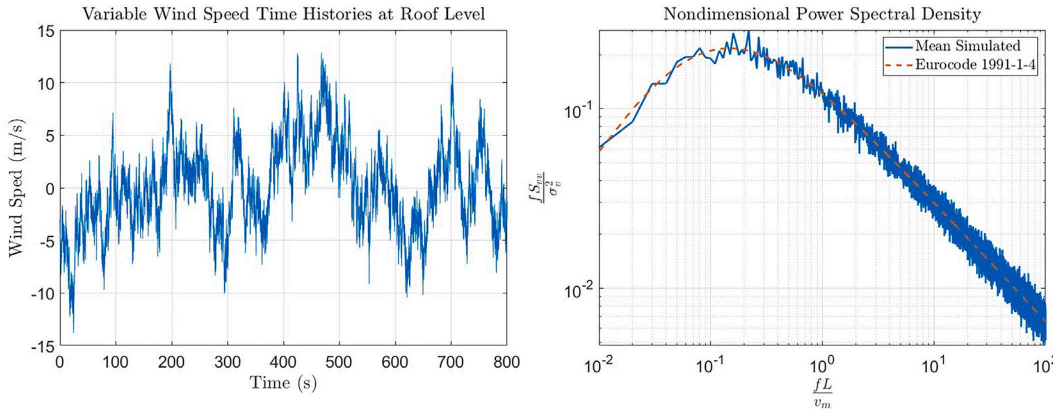

Fig. 4. Example power spectral density and time history of generated variable wind speed for the top storey for a basic wind velocity of $15 m/s$.

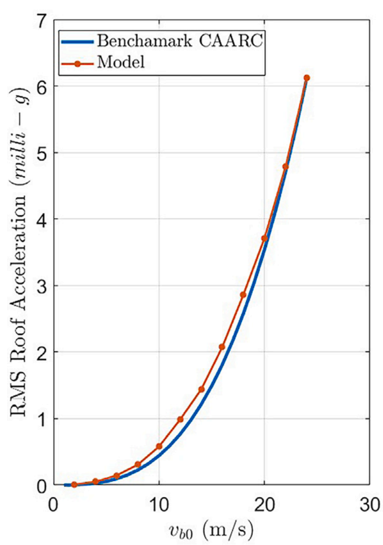

Fig. 5. Comparison of along wind RMS roof acceleration from aeroelastic wind tunnel [51] testing and numerical model for the CAARC building.

In light of this, two different sets of distributions are employed to represent the modal properties of the building. For the first distribution, termed the 'uninformed case', natural frequency and modal damping are assumed to be normally distributed with mean values taken from the closed form expressions given in Eurocode 1991-1-4 [44]; this corresponds to a mean fundamental frequency, F_1, of $Height/46 = Hz$, and a mean damping value, ζ_1 of 1.27%. The coefficients of variation (CoV) are assumed to be 25% and 50% respectively; this aligns with the recommended values proposed by Picozzi et al. based on comprehensive analysis of various predictive models for the dynamic properties of tall buildings [55]. These distributions represent the knowledge of the structure during the initial stages of the design process, prior to construction and further information becoming available.

A second distribution, termed the 'data-informed case', is developed using modal properties identified from ambient acceleration data recorded from in-situ monitoring of *Ten Degrees*. The natural frequency and damping ratio of the building in the first mode were obtained through the application of a Bayesian Fast Fourier Transform (BFFT) [56,57] Operational Modal Analysis (OMA) approach as discussed in [19]. The reader is referred to [19,21] for a full description of the structural form and design of *Ten Degrees* and analysis of the in-situ results. From this OMA approach, the mean natural frequency was identified as $0.313 Hz$, with a standard deviation of $0.0045\ Hz$, which corresponds to a coefficient of variation of 1.5%. Similarly, the mean modal damping ratio was identified as 1.33% with a standard deviation of 0.12%, which corresponds to a coefficient of variation of 9.1%. It can be appreciated from the coefficients of variation and Fig. 11 that the extent of the epistemic uncertainty is substantially reduced in the data-informed case. This is particularly true for the natural frequency which can be identified with high precision from OMA. Consideration of both the 'uninformed' and 'data-informed' cases is important as the ability to assess the benefit of auxiliary damping is dependent on the state of knowledge of the structure.

In the case of *Ten Degrees*, in-situ monitoring showed that FE models underestimated the natural frequency of the structure substantially [21]. This highlights the necessity for improved data-informed models that more accurately reflect the dynamic properties of modular buildings.

2.6. Numerical simulation and effectiveness of multiple vertically distributed tuned liquid dampers

The reduced-order model is used to perform simulations to investigate the effectiveness of MVDTLDs in reducing the dynamic response of modular buildings where uncertainty surrounds the inherent dynamic properties. In order to do this, analysis is performed for the structure with three different auxiliary damping strategies; namely a baseline case with no auxiliary damping, a conventional approach with TLDs located at roof level, and a case with MVDTLDs distributed over the top third of the building. Furthermore, analysis is performed considering representations of modal properties corresponding to the 'uninformed case' and the 'data-informed case'. Thus, overall, six analysis cases are considered. This allows the impact of various auxiliary damping approaches on habitability to be assessed given different levels of epistemic uncertainty as the design progresses.

As discussed, the building parameters and dynamic properties used in the data-informed surrogate model reflect those of *Ten Degrees* as detailed in Table 2.

3. Development of fragility curves

A fragility analysis has been performed to further investigate the effectiveness of MVDTLDs in improving the reliability of high-rise modular buildings. Fragility curves have been widely used across wind and earthquake engineering to assess the probability of exceeding prescribed limit states (for example by [40,58,59] amongst others). Fragility curves are a useful tool for relating the probability of exceeding prescribed damage state thresholds to a chosen wind speed interval [43]. A nested loop approach is adopted to separately consider aleatory and epistemic uncertainty in the development of the fragility curves, as illustrated in Fig. 6 and discussed in the following sections.

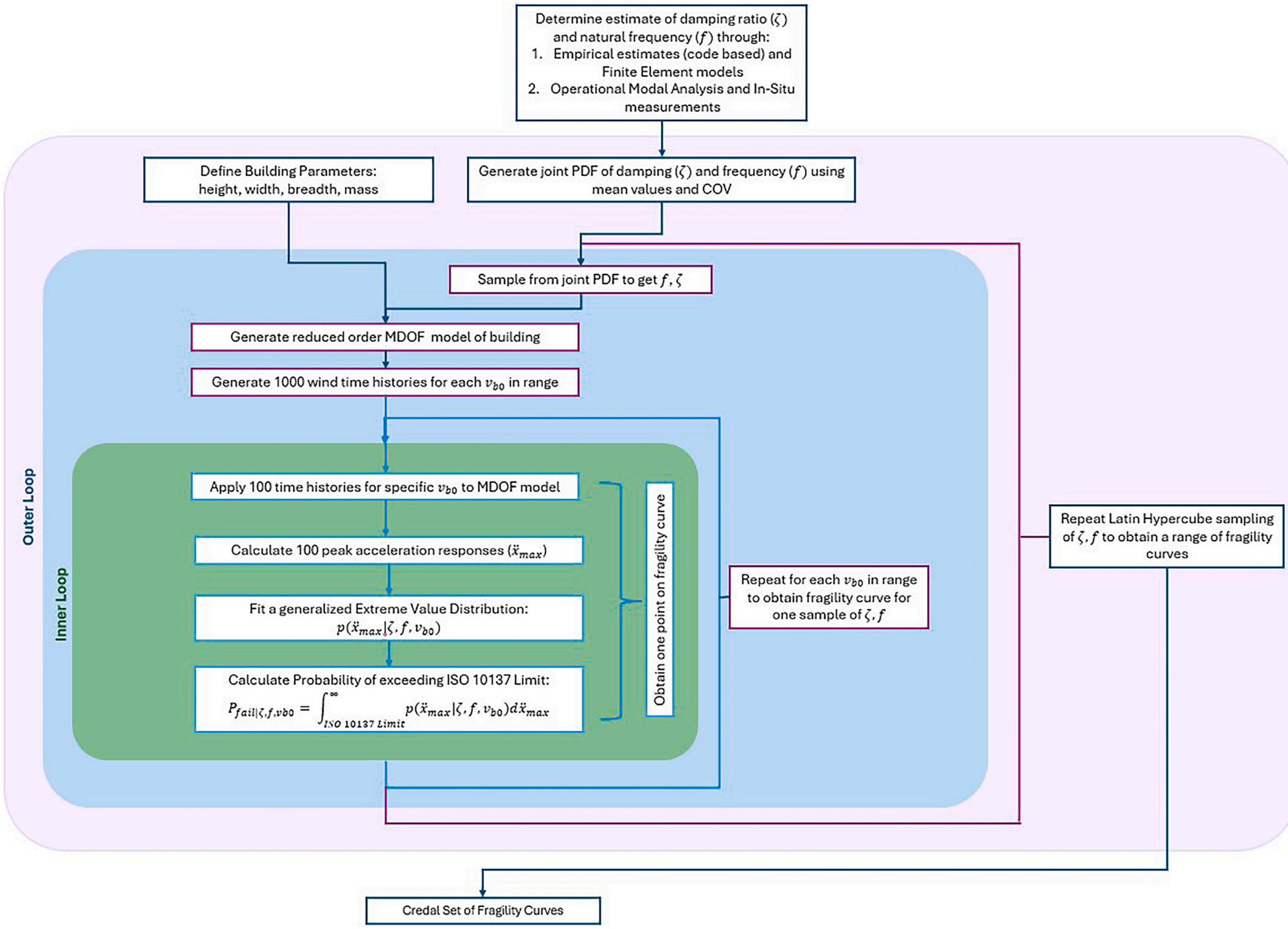

Fig. 6. Flow chart explaining the nested loop methodology followed in the development of the fragility curves.

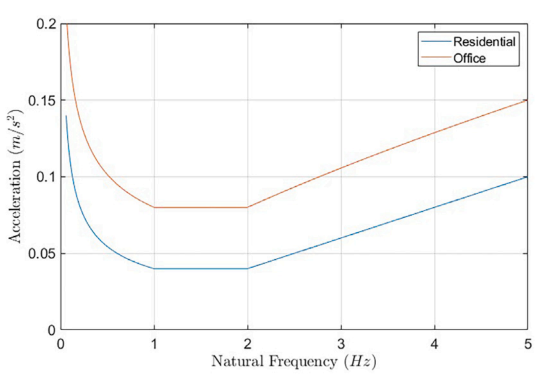

Fig. 7. ISO 10,137 peak acceleration limits [9].

3.1. Damage state definition

The acceleration thresholds chosen to construct the fragility curves are based on peak acceleration limits defined by the International Organisation for Standardisation (ISO). ISO 10,137 imposes serviceability limits on peak acceleration for a 1 in 1 year wind event for both residential and commercial buildings. ISO 10,137 [9] limits for residential buildings are used as the damage state in this study and are presented in Fig. 7. These criteria are based on accelerations that are disruptive to approximately 2% of the people occupying the upper third of the building.

3.2. Aleatory failure probability

As mentioned, aleatory and epistemic uncertainties are considered separately through a nested sampling approach in analysis, illustrated in Fig. 6, with aleatory uncertainty considered within the inner sampling loop. For a given mean wind speed value, v_{b0} and combination of fundamental frequency and damping, time history analysis is performed using 100 samples of variable wind time histories which are generated as described in Section 2.3. This sample approximates the aleatory uncertainty present due to the stochastic wind excitation. The peak absolute acceleration response over 10 minutes is recorded for each sampled wind speed time history. A generalized extreme value distribution is fitted to this set of peak responses. This represents the aleatory probability density of peak acceleration for a given combination of frequency damping and mean wind speed, $p(\ddot{x}|f_1, \zeta_1, v_{b0})$. Using this distribution, the conditional aleatory probability of exceeding the limit state defined by ISO 10137, $P(\ddot{x} > \ddot{x}_{ISO}|f_1, \zeta_1, v_{b0})$, can be estimated through Eq. (25):

$$P(\ddot{x} > \ddot{x}_{ISO}|f_1, \zeta_1, v_{b0}) = \int_{\ddot{x}_{iso}}^{\infty} p(\ddot{x}|f_1, \zeta_1, v_{b0}) \mathrm{d}\ddot{x} \quad (25)$$

where P denotes a probability and p is a probability density.

3.3. Epistemic failure probability

Epistemic uncertainty is considered in the outer loop, where 100 samples of fundamental frequency and damping are taken from the distribution under consideration, which is either the ‘uninformed’ or

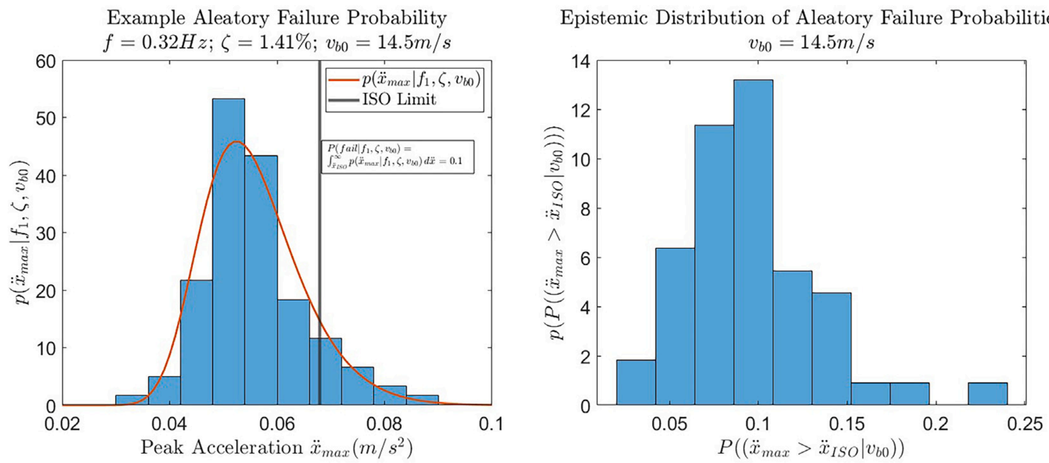

Fig. 8. Example for a mean wind speed of $14.5m/s$ from the data-informed, no TLD scenario showing (a) the distribution of peak acceleration and calculated aleatory failure probability for a set fundamental frequency and damping combination and (b) the epistemic distribution of aleatory failure probabilities across 100 combinations of fundamental frequency and damping.

'data-informed' case. The analysis to evaluate aleatory failure probability is repeated for each of these samples. This gives a distribution of failure probabilities across the epistemically uncertain parameters.

These concepts are illustrated in Fig. 8 for a mean wind speed of $14.5m/s$ for the 'data-informed' no TLD scenario. The left-hand subfigure shows the result of the inner loop for a single example combination of fundamental frequency and damping. It shows the histogram (normalized to a unit area) of peak acceleration obtained from analysis of 100 variable wind speed time histories, the fitted generalized extreme value distribution and calculation of aleatory failure probability through Eq. (25). The right-hand subfigure displays the result of the outer loop; which is a histogram of these aleatory failure probabilities across 100 different combinations of fundamental frequency and damping (i.e. obtained by repeating the analysis in the left-hand subfigure 100 times). This shows the epistemic distribution of aleatory failure probabilities for the given wind speed and analysis case.

3.4. Development of fragility curves

The analysis presented in Fig. 8 gives a distribution of aleatory failure probabilities, $P(\ddot{x} > \ddot{x}_{ISO}|v_b 0))$ for a given mean wind speed. A fragility curve can then be developed by considering the variation in aleatory failure probability across a range of mean wind speed values. Other studies that explicitly consider both aleatory and epistemic uncertainty in fragility analysis have done this by combining these two forms of uncertainty prior to fitting the fragility curve for example through approaches based on the square root of sums squares or the total probability theorem (e.g. [60,61]). However, while this approach is common in earthquake engineering in particular, the logical consistency and validity of combining epistemic and aleatory uncertainties is sometimes questioned in literature (e.g. [62–65]). In light of this, in this study a set of fragility curves are fitted to the aleatory failure probabilities through a quantile regression without combining aleatory and epistemic probabilities. In this process it is assumed that the fragility curve at each quantile can be represented by a cumulative lognormal distribution, as is typically assumed in fragility analysis. This idea is illustrated in Fig. 9, which shows an example of the set of fragility curves being constructed for the data-informed MVDTLD case. From the figure it can firstly be appreciated how the fragility curves are developed from a set of epistemic distributions of failure probabilities at a series of mean wind speeds, similar to the one shown in right-hand subfigure in Fig. 8. Additionally, it can also be appreciated how the fragility curves from quantile regression can be used to represent the spread of epistemic uncertainty in the failure probability; with fitted fragility curves representing the median (i.e.

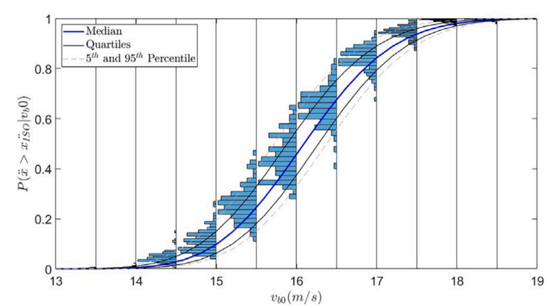

Fig. 9. Example showing the epistemic uncertainty associated with $P(fail|v_{b0})$ and the median, quartiles, 5th and 95th percentile fragility curves for the data-informed MVDTLD case.

50th percentile), quartiles (i.e. 25th and 75th percentiles), and 5th and 95th percentiles all shown. Presenting the fragility curves in this way allows the epistemic uncertainty in the aleatory failure probability to be examined, providing further insight into the contributions of different uncertainties to the overall failure probability.

4. Results

The calculated fragility curves for the six cases considered (uninformed and data-informed, with no TLD, a TLD at roof level and MVDTLDs) are shown in Fig. 10. The median fragility curve, the fragility curves representing the inter-quartile range (i.e., the 25th and 75th percentiles) and the fragility curves representing the 90th percentile interval (i.e. the 5th and 95th percentiles) are presented for each case. It can be instantly appreciated from the much smaller inter-quartile range that the epistemic uncertainty is greatly reduced for the three data-informed cases. This is as expected given the substantial reduction in the coefficients of variation of fundamental frequency and damping.

Fig. 11 presents the median fragility curves from each of the six cases on one plot for ease of comparison. Firstly, at a high level, the median fragility curves are broadly similar; all suggest that the acceleration will exceed habitability requirements for a mean wind speed somewhere between $14m/s$ and $18m/s$, irrespective of the epistemic uncertainty or auxiliary damping strategy employed. However, the two right-most fragility curves, and therefore the scenarios with the lowest probability of failure, are the two scenarios where MVDTLDs are employed. These are followed by the case where a single TLD is placed at roof level for the

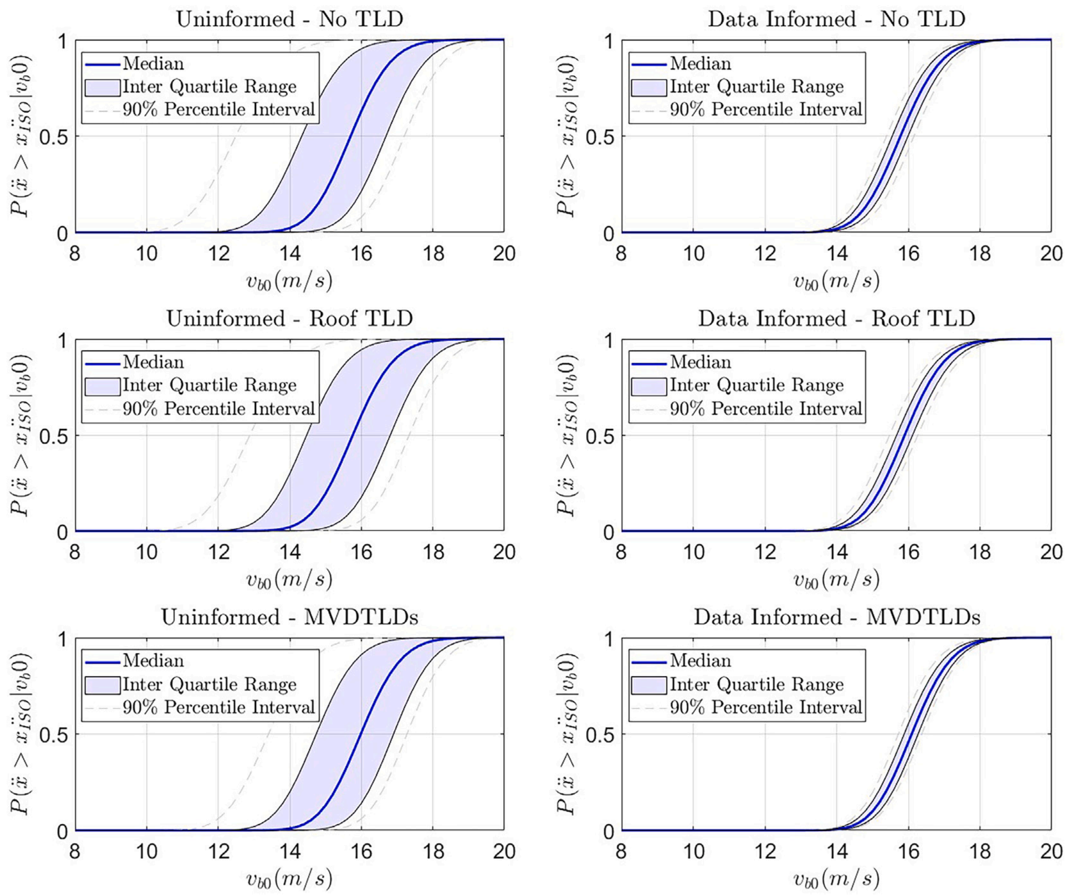

Fig. 10. Fragility curves showing probability of peak acceleration exceeding the ISO 10,137 habitability limits for the six cases considered.

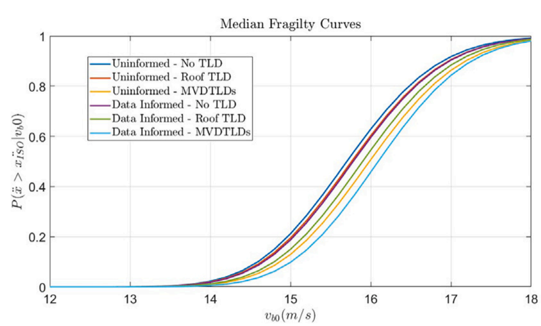

Fig. 11. Median fragility curves from the 6 cases considered.

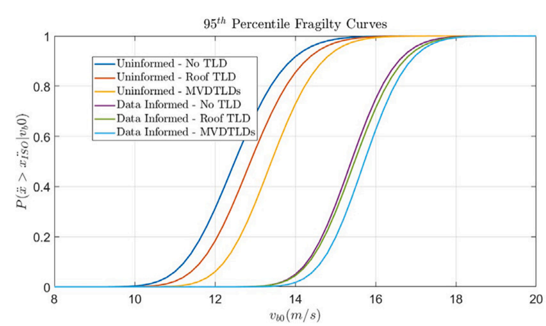

Fig. 12. 95th percentile fragility curves.

'data-informed' representation of epistemic uncertainty. The curves for the 'data-informed' case with no auxiliary damping and the 'uninformed' case with a TLD at roof level are very similar to the extent that they are almost indistinguishable. Finally, the left-most curve is the 'uninformed' case with no TLD. In some respects these results are as expected; predictably, the addition of auxiliary damping moves the curves to the right, showing that auxiliary damping devices increase the wind speed at which the limit state will be exceeded. However, the fact that the curves for the MVDTLDs are the two right-most curves is a less predictable result. This suggests that the MVDTLD approach is more effective than the conventional placement of an equivalent TLD system with the same overall mass ratio at the roof. Furthermore, the fact that the MVDTLD curve for the 'uninformed' case is further right than the 'data-informed' TLD curve suggests that MVDTLDs represent an effective way to control performance in the presence of substantial epistemic uncertainty.

The idea that MVDTLDs are an effective mitigation strategy under uncertainty is reinforced by examining the 95th percentile fragility curves, which are compared for each of the six cases on one plot in Fig. 12. These 95th percentile curves can be informally considered as a representation of the 'reasonable worst case scenario' for a given level of epistemic uncertainty. As with the median curves, some of the trends observed here are to be expected. Firstly, the 'data-informed' curves are much further right than the 'uninformed' curves. This is a result of the reduced epistemic uncertainty greatly reducing the possibility of poorly performing low-damping low-frequency combinations. Secondly, the curves with auxiliary damping are predictably further right than the comparable curves with no TLDs, again demonstrating the well-known fact that auxiliary damping is beneficial. However, less-predictably, again the MVDTLD curves are further right than the comparable conventional TLD curves. This shows that for the example case considered the MVDTLDs offer better mitigation against excessive acceleration than conventional TLDs at roof level. Additionally, the shift to the right offered by the MVDTLD in the uninformed case is particularly pronounced. The results suggest that for the case with no auxiliary damping, failure is possible at mean basic wind speeds as low as $10m/s$. However, MVDTLDs almost eliminate the possibility of failure at mean wind speeds below $12m/s$. Therefore, it can be concluded that for the considered structure, MVDTLDs offer the most benefit at the critical tail of the epistemic distribution and are most effective at preventing failure at lower, more frequently occurring, mean wind speeds.

Whilst the analysis performed within this paper considers one case study building alone, in a wider context the results suggest that MVDTLDs have the potential to out-perform conventional TLDs, particularly at the critical tail of the distribution of epistemic uncertainty. This is an especially relevant finding for volumetric modular buildings for two primary reasons. Firstly, the repetitive nature of the fabrication process makes an MVDTLD strategy more realistic and feasible than in conventional construction. Secondly, the novel nature of modular construction and the very limited number of field studies on tall modular structures result in an inherently high level of epistemic uncertainty associated with their modal properties, meaning a design solution that offers improved performance under uncertainty is attractive. However, having said this, care should be taken when extrapolating the conclusions beyond the case study scenario considered and further work considering a much wider range of archetype structures is needed to generalize these conclusions. There is also a need to consider the limitations of the current study, which are primarily related to the simplifying assumptions made in the development of the reduced-order model. These include neglecting higher modes of vibration, neglecting non-linear effects of liquid sloshing in the TLDs through the equivalent TMD assumption, and the restriction of analysis to along wind response. These assumptions facilitate computational efficiency and allow for a large number of analyses to be performed to assess the impact of uncertainty. However, there is a need to investigate the impact of these assumptions on the key conclusions.

5. Conclusions

A set of fragility curves capturing epistemic uncertainty in modal properties has been used to explore the improvement in the reliability of high-rise modular buildings with uncertain inherent dynamic properties where MVDTLDs are employed. The reliability is assessed with respect to serviceability limits related to occupant comfort set out by ISO 10,137. A reduced-order model was created using structural properties of one of Europe's tallest modular buildings, *Ten Degrees*. Analysis is performed for six different cases, considering no auxiliary damping, TLDs at roof level and MVDTLDs for two different levels of epistemic uncertainty; an 'uninformed' case representing the state of knowledge prior to monitoring and modal identification and a 'data-informed' case using modal properties obtained from operational modal analysis.

The fragility curves demonstrate the effectiveness of MVDTLDs in controlling the dynamic response of the modular building under consideration. In all cases, the performance of MVDTLDs was superior to the conventional strategy of locating TLDs at roof level only. The biggest performance benefit of MVDTLDs was observed for the 95th percentile fragility curve, suggesting they offer the most benefit at the critical tail of the epistemic distribution. Therefore, overall, the results presented suggest that the reliability of modular buildings can be improved through addition of MVDTLDs and that MVDTLDs may be a particularly attractive auxiliary damping strategy for modular buildings if the decision to employ auxiliary damping is required prior to the availability of data to reduce epistemic uncertainty.

CRediT authorship contribution statement

Hollie Moore: Writing – original draft, Formal analysis, Data curation, Conceptualization. **Brian Broderick:** Writing – review & editing, Supervision, Funding acquisition. **Breiffni Fitzgerald:** Writing – review & editing, Supervision, Funding acquisition. **John Hickey:** Writing – review & editing, Writing – original draft, Formal analysis.

Declaration of competing interest

The authors declare that they have no known competing financial interests or personal relationships that could have appeared to influence the work reported in this paper.

Acknowledgements

Funding for this research was provided by the Irish Government through the Irish Research Council [Grant No. EBPPG/2020/244] and by Barrett Mahony Consulting Engineers. Information and data collection for this research was facilitated and supplied by Tide Construction. The authors also wish to thank Shane Linehan and Vincent Barrett at Barrett Mahony Consulting Engineers for their support in this work, as well as the anonymous reviewers whose comments greatly improved the manuscript.

Data availability

All code used to generate figures and data in this paper can be found at the following link: https://github.com/hickeyj2/FragilityAnalysis_HighRiseModular_MVDTLDs.

References

[1] Lawson M, Ogden R, Goodier C. Design in modular construction. CRC Press; 2014.
[2] Chen Z, Khan K, Khan A, Javed K, Liu J. Exploration of the multidirectional stability and response of prefabricated volumetric modular steel structures. J Constr Steel Res 2021. [Online]. Available: 184:106826. https://www.sciencedirect.com/science/article/pii/S0143974X21003084.
[3] Thai H-T, Ngo T, Uy B. A review on modular construction for high-rise buildings. Structures 2020. [Online]. Available: 28:1265–90. https://www.sciencedirect.com/science/article/pii/S2352012420305476.
[4] Gunawardena T, Ngo T, Mendis P, Alfano J. Innovative flexible structural system using prefabricated modules. J Archit Eng 2016. [Online]. Available: 22(4):05016003. https://doi.org/10.1061/(ASCE)AE.1943-5568.0000214
[5] Moore H, Hickey J, Broderick B, Fitzgerald B. Damping ratio identification of a volumetric modular high-rise building. Eng Struct 2026. [Online]. Available: 352:122011. https://www.sciencedirect.com/science/article/pii/S0141029625024022.
[6] Moore H, Hickey J, Fitzgerald B, Broderick B. Signal processing of acceleration responses for damping ratio identification of a high-rise modular building. Ifac-pap 2025, 17th IFAC Symposium on Large Scale Complex Systems: Theory and Applications LSS 2025. [Online]. Available: 59(21):13–18. https://www.sciencedirect.com/science/article/pii/S2405896325022621.
[7] Fu J, Zheng Q, Huang Y, Wu J, Pi Y, Liu Q. Design optimization on high-rise buildings considering occupant comfort reliability and joint distribution of wind speed and direction. Eng Struct 2018. [Online]. Available: 156:460–71. http://www.sciencedirect.com/science/article/pii/S0141029617319880https://www.sciencedirect.com/science/article/abs/pii/S0141029617319880?via%3Dihub.
[8] Kwok KCS, Hitchcock PA, Burton MD. Perception of vibration and occupant comfort in wind-excited tall buildings. J Wind Eng Ind Aerodyn 2009. [Online]. Available: 97(7):368–80. https://www.sciencedirect.com/science/article/pii/S0167610509000373.
[9] ISO 10137: Basis for design structures: serviceability of buildings and walkways against vibrations. 2007. [Online]. Available: British Standard https://books.google.ie/books?id=nYWzzQEACAAJ.
[10] Burton MD, Kwok KC, Abdelrazaq A. Wind-induced motion of tall buildings: designing for occupant comfort. Int J High-Rise Build 2015;4(1):1–8.
[11] Lacey AW, Chen W, Hao H, Bi K. Structural response of modular buildings – an overview. J Build Eng 2018. [Online]. Available: 16:45–56. http://www.sciencedirect.com/science/article/pii/S2352710217303650.
[12] Liew JYR, Chua YS, Dai Z. Steel concrete composite systems for modular construction of high-rise buildings. Structures 2019. [Online]. Available: 21:135–49. https://www.sciencedirect.com/science/article/pii/S2352012419300347.
[13] Sivandi-Pour A, Gerami M, Kheyroddin A. Uniform damping ratio for non-classically damped hybrid steel concrete structures. Int J Civ Eng 2016. [Online]. Available: 14(1):1–11. https://doi.org/10.1007/s40999-016-0003-8
[14] Chua YS, Liew JYR, Pang SD. Modelling of connections and lateral behavior of high-rise modular steel buildings. J Constr Steel Res 2020. [Online]. Available: 166:105901. https://www.sciencedirect.com/science/article/pii/S0143974X19302044.
[15] Lacey AW, Chen W, Hao H, Bi K. Lateral behaviour of modular steel building with simplified models of new inter-module connections. Eng Struct 2021. [Online]. Available: 236:112103. https://www.sciencedirect.com/science/article/pii/S0141029621002534.

[16] Kijewski-Correa T, Kilpatrick J, Kareem A, Kwon D-K, Bashor R, Kochly M, Young BS, Abdelrazaq A, Galsworthy J, Isyumov N. Validating wind-induced response of tall buildings: synopsis of the Chicago full-scale monitoring program. J Struct Eng 2006. [Online]. Available: 132(10):1509–23. https://ascelibrary.org/doi/abs/10.1061/%28ASCE%290733-9445%282006%29132%3A10%281509%29.

[17] Feng Z, Zhao B, Hua X, Chen Z, Asce M. Enhanced EMD-RDT method for output-only ambient modal identification of structures. J Aerosp Eng 2019. [Online]. Available: 32:04019046. https://ascelibrary.org/doi/abs/10.1061/%28ASCE%29AS.1943-5525.0001034.

[18] Ivanovic SS, Trifunac MD, Todorovska M. Ambient vibration tests of structures-a review. ISET J earthq Technol 2000. [Online]. Available: 37(4):165–97. https://doi.org/10.63898/DZXP4400

[19] Hickey J, Moore H, Broderick B, Fitzgerald B. Structural damping estimation from live monitoring of a tall modular building. Struct Des Tall Spec Build 2024. [Online]. Available: 33(1):e2067. https://onlinelibrary.wiley.com/doi/abs/10.1002/tal.2067.

[20] Barrett Mahony Consulting Engineers. Ten degrees Croydon; 2025. [Online]. Available: https://www.barrettmahony.com/projects/ten-degrees-croydon/ [Accessed: 23 July 2025].

[21] Moore H, Hickey J, Broderick B, Fitzgerald B, Barrett V, Linehan S. Wind-induced vibration response of modular high-rise buildings. Struct Eng May 2025. [Online]. Available: 103(5):8–10. https://www.istructe.org/journal/volumes/volume-103-(2025)/issue-5/wind-induced-vibration-response-of-modular/.

[22] Kareem A, Sun WJ. Stochastic response of structures with fluid-containing appendages. J Sound Vib 1987. [Online]. Available: 119(3):389–408. https://www.sciencedirect.com/science/article/pii/0022460X87904056.

[23] Fujino Y, Sun L, Pacheco Benito M, Chaiseri P. Tuned liquid damper (TLD) for suppressing horizontal motion of structures. J Eng Mech 1992. [Online]. Available: 118(10):2017–30. https://doi.org/10.1061/(ASCE)0733-9399(1992)118:10(2017)

[24] Jin H, Calabrese A, Liu Y. Effects of different damping baffle configurations on the dynamic response of a liquid tank under seismic excitation. Eng Struct 2021. [Online]. Available: 229:111652. http://www.sciencedirect.com/science/article/pii/S014102962034253X.

[25] Love JS, Tait MJ. Parametric depth ratio study on tuned liquid dampers: fluid modelling and experimental work. Comput Fluids 2013. [Online]. Available: 79:13–26. https://www.sciencedirect.com/science/article/pii/S0045793013000935.

[26] Soliman IM, Tait MJ, El Damatty AA. Development and validation of finite element structure-tuned liquid damper system models. J Dyn Syst Meas Control 2015. [Online]. Available: 137(11). https://doi.org/10.1115/1.4030866

[27] Konar T, Ghosh AD. Flow damping devices in tuned liquid damper for structural vibration control: a review. Arch Comput Methods Eng 2021. [Online]. Available: 28(4):2195–207. https://link.springer.com/content/pdf/10.1007/s11831-020-09450-0.pdf.

[28] Love JS, Morava B, Robinson JK, Haskett TC. Tuned sloshing dampers in tall buildings: a practical performance-based design approach. Pract Period Struct Des Constr 2021. [Online]. Available: 26(3). https://doi.org/10.1061/(asce)sc.1943-5576.0000582

[29] Vern S, Shrimali MK, Bharti SD, Datta TK. Optimum seismic control and safety measures in liquid storage tanks by the amalgamation of different passive control devices. J Perform Constr Facil 2022. [Online]. Available: 36(3):04022026. https://ascelibrary.org/doi/abs/10.1061/%28ASCE%29CF.1943-5509.0001735.

[30] Collins R. Vibration control of structures using active and semi-active tuned mass dampers, PhD, [Online]. Available: 2005. http://hdl.handle.net/2262/86680.

[31] Fujino Y, Sun LM. Vibration control by multiple tuned liquid dampers (MTLDs). J Struct Eng 1993. [Online]. Available: 119(12):3482–502. https://doi.org/10.1061/(ASCE)0733-9445(1993)119:12(3482)

[32] Igusa T, Xu K. Vibration control using multiple tuned mass dampers. J Sound Vib 1994. [Online]. Available: 175(4):491–503. https://www.sciencedirect.com/science/article/pii/S0022460X84713411.

[33] Kareem A, Kline S. Performance of multiple mass dampers under random loading. J Struct Eng 1995. [Online]. Available: 121(2):348–61. https://doi.org/10.1061/(ASCE)0733-9445(1995)121:2(348)

[34] Elias S, Matsagar V, Datta TK. Dynamic response control of a wind-excited tall building with distributed multiple tuned mass dampers. Int J Struct Stab Dyn 2019. [Online]. Available: 19(6):1950059. https://doi.org/10.1142/S0219455419500597

[35] Ozturk B, Cetin H, Aydin E. Optimum vertical location and design of multiple tuned mass dampers under seismic excitations. Structures 2022. [Online]. Available: 41:1141–63. https://www.sciencedirect.com/science/article/pii/S2352012422003757.

[36] Moon KS. Vertically distributed multiple tuned mass dampers in tall buildings: performance analysis and preliminary design. Struct Des Tall Spec Build 2010. [Online]. Available: 19(3):347–66. https://doi.org/10.1002/tal.499

[37] Tait MJ. Modelling and preliminary design of a structure-TLD system. Eng Struct 2008. [Online]. Available: 30(10):2644–55. http://www.sciencedirect.com/science/article/pii/S0141029608000667.

[38] Hickey J, Broderick B, Fitzgerald B, Moore H. Mitigation of wind induced accelerations in tall modular buildings. Structures 2022. [Online]. Available: 37:576–87. https://www.sciencedirect.com/science/article/pii/S2352012422000376.

[39] Tamura Y, Yoshida A. Amplitude dependency of damping in buildings. In: Structures congress 2008; 2008. p. 1–10. [Online]. Available: https://doi.org/10.1061/41000(315)39

[40] Nava-González R, Pozos-Estrada A, López-Ibarra A. Development of fragility curves for tall buildings with tuned liquid dampers for vibration control under wind loading. Int J Civ Eng 2024. [Online]. Available: https://doi.org/10.1007/s40999-024-01020-w

[41] Greco A, Caddemi S, Caliò I, Fiore I. A review of simplified numerical beam-like models of multi-storey framed buildings. Buildings 2022. [Online]. Available: 12(9). https://www.mdpi.com/2075-5309/12/9/1397.

[42] Chen X. Analysis of alongwind tall building response to transient nonstationary winds. J Struct Eng 2008;134(5):782–91.

[43] Smith MA, Caracoglia L. A Monte Carlo based method for the dynamic fragility analysis" of tall buildings under turbulent wind loading. Eng Struct 2011. [Online]. Available: 33(2):410–20. https://www.sciencedirect.com/science/article/pii/S0141029610004189.

[44] Eurocode 1: actions on structures - Part 1-4: General actions - wind actions. 2004, no. EN 1991-1-4:2005. [Online]. Available: European Committee for Stadarization https://eurocodes.jrc.ec.europa.eu/EN-Eurocodes/eurocode-1-actions-structures.

[45] Sun LM, Fujino Y, Chaiseri P, Pacheco BM. The properties of tuned liquid dampers using a TMD analogy. Earthq Eng Struct Dyn 1995. [Online]. Available: 24(7):967–76. https://doi.org/10.1002/eqe.4290240704

[46] Tait MJ, Deng X. The performance of structure-tuned liquid damper systems with different tank geometries. Struct Control Health Monit, pp. n/a–n/a, 2008. [Online]. Available: https://doi.org/10.1002/stc.286

[47] Tamura Y. Application of damping devices to suppress wind-induced responses of buildings. J Wind Eng Ind Aerodyn 1998. [Online]. Available: 74-76:49–72. https://www.sciencedirect.com/science/article/pii/S0167610598000063.

[48] Elias S, Matsagar V. Wind response control of 76-storey benchmark building with distributed multiple tuned mass dampers. In: Iyer N, Krishna P, Selvi R, Harikrishna P, editors. Proceedings of the 8th Asia-Pacific conference on wind engineering, APCWE 2013. Research Publishing Services; 2013. p. 968–77.

[49] Elias S, Matsagar V, Datta T. Distributed multiple tuned mass dampers for wind response control of chimney with flexible foundation. Procedia Eng 2017, X International Conference on Structural Dynamics, EURODYN 2017. [Online]. Available: 199:1641–6. https://www.sciencedirect.com/science/article/pii/S1877705817335233.

[50] Wittig LE, Sinha AK. Simulation of multicorrelated random processes using the FFT algorithm. J Acoust Soc Am Sep 1975. [Online]. Available: 58(3):630–4. https://doi.org/10.1121/1.380702

[51] Melbourne W. Comparison of measurements on the caarc standard tall building model in simulated model wind flows. J Wind Eng Ind Aerodyn 1980;6(1–2):73–88.

[52] Obasaju E. Measurement of forces and base overturning moments on the CAARC tall building model in a simulated atmospheric boundary layer. J Wind Eng Ind Aerodyn 1992;40(2):103–26.

[53] Zhang Y, Habashi WG, Khurram RA. Predicting wind-induced vibrations of high-rise buildings using unsteady CFD and modal analysis. J Wind Eng Ind Aerodyn 2015;136:165–79.

[54] Verma H, Sonparote R. Forecasting of pressure coefficient for wind interference due to surrounding tall building on a tall rectangular building using CFD data trained machine learning models. In: Structures, 75. Elsevier; 2025, p. 108705.

[55] Picozzi V, Maietta V, Avossa AM, Ricciardelli F. Uncertainty in the dynamic properties of tall buildings and propagation to the wind-induced response. Struct Des Tall Spec Build 2024;33(10):e2107.

[56] Yuen K-V, Katafygiotis LS. Bayesian fast Fourier transform approach for modal updating using ambient data. Adv Struct Eng 2003;6(2):81–95.

[57] Au S-K. Fast Bayesian FFT method for ambient modal identification with separated modes. J Eng Mech 2011;137(3):214–26.

[58] Fitzgerald B, Sarkar S, Staino A. Improved reliability of wind turbine towers with active tuned mass dampers (ATMDs). J Sound Vib Apr 2018. [Online]. Available: 419:103–22. https://ui.adsabs.harvard.edu/abs/2018JSV...419..103F.

[59] Sharma V, Shrimali MK, Bharti SD, Datta TK. Seismic fragility evaluation of semi-rigid frames subjected to near-field earthquakes. J Constr Steel Res 2021. [Online]. Available: 176:106384. https://www.sciencedirect.com/science/article/pii/S0143974X20309366.

[60] Su L, Li X-L, Jiang Y-P. Comparison of methodologies for seismic fragility analysis of unreinforced masonry buildings considering epistemic uncertainty. Eng Struct 2020;205:110059.

[61] Kim J, Kim T. Efficient seismic fragility analysis considering uncertainties in structural systems and ground motions. Earthq Eng Struct Dyn 2025;54(1):206–26.

[62] Ferson S, Ginzburg LR. Different methods are needed to propagate ignorance and variability. Reliab Eng Syst Saf 1996;54(2–3):133–44.

[63] Der Kiureghian A, Ditlevsen O. Aleatory or epistemic? Does it matter? Struct Saf 2009;31(2):105–12.

[64] Mullins J, Ling Y, Mahadevan S, Sun L, Strachan A. Separation of aleatory and epistemic uncertainty in probabilistic model validation. Reliab Eng Syst Saf 2016;147:49–59.

[65] Hickey J, Langley R. Alternative metrics for design decisions based on separating aleatory and epistemic probabilistic uncertainties. Mech Syst Signal Process 2022;181:109532.